Dual-axis video observations of ice crushing utilizing high-speed video for one perspective

Gagnon, R. E.; Daley, C.

18th International Conference on Port and Ocean Engineering Under Arctic Conditions [Proceedings], 2005

Proc., 18th Int. Conf. on Port and Ocean Eng. Under Arctic Conditions, Vol. I (2005) 271-282

DUAL-AXIS VIDEO OBSERVATIONS OF ICE CRUSHING UTILIZING HIGH-SPEED VIDEO FOR ONE PERSPECTIVE

R.E. Gagnon[1] and Claude Daley[2]

[1]Institute for Ocean Technology
National Research Council of Canada
St. John's, NL, Canada, A1B 3T5

[2]Faculty of Engineering and Applied Science
Memorial University of Newfoundland
St. John's, NF, A1B 3X5

ABSTRACT

Rectangular thick sections (1 cm thickness) of lab-grown monocrystalline ice have been confined between two thick Plexiglas plates and crushed at –10°C from one edge face at a rate of 1 cm/s using a transparent Plexiglas platen (1 cm thickness) inserted between the plates. The transparent plates and platen permitted side viewing of the ice behavior during crushing using high-speed video and also a top view of the ice/platen contact zone through the crushing platen using regular video. Zones of intact ice at the ice / platen interface were evident in the visual records and these were shaped by cracks and spalls. The production and flow of liquid in a thin layer at the intact ice / platen interface was also evident. A novel method was used to obtain pressure measurements at the ice/platen interface. Pressure values for the intact ice contact zones were high (at least 30 MPa) and for the crushed ice the pressure varied from low (< 5 MPa) to high values (~ 30 MPa) depending on its thickness over intact ice. Also, wetting from liquid produced at the intact ice / platen interface probably softened and reduced the pressure in pulverized ice. Features of the load and pressure data are discussed in the context of the visual observations.

INTRODUCTION

Several studies of ice crushing behavior have been conducted over of the past few decades. Some of the more recent investigations included in situ visual observations using indentors (Joensuu and Riska, 1988, Muhonen 1991; Gagnon, 1998; Fransson et al., 1991) and a ship hull (Riska et al., 1990) that incorporated windows for viewing the indented ice surface. There have also been test apparatus that allowed viewing of the ice/indentor interface through the ice samples (Gagnon, 1994a; Gagnon and Mølgaard, 1991). These have lead to significant new insights into the ice crushing process.

The present study incorporates a similar concept to that of Wilson (1999), except that the strain rate is much higher, and is in the range associated with ice crushing rather than plastic deformation. The loads are much higher and the apparatus is correspondingly stronger. Experiments similar to the present ones have been performed by Gagnon (2004).

METHOD AND APPARATUS

Figure 1a shows a conceptual schematic of the test method. The ice specimen is a 1 cm thick section. The sample is confined between two thick plates (12 cm x 13 cm x 3.8 cm) of transparent Plexiglas. The Plexiglas plates are mounted in a holder (Figure 1b), made from 19 mm thick Aluminum plate, that keeps the Plexiglas and ice specimen in place. The Plexiglas plates are separated by small plastic spacers (1 cm thick) between the plates at the sides. The holder

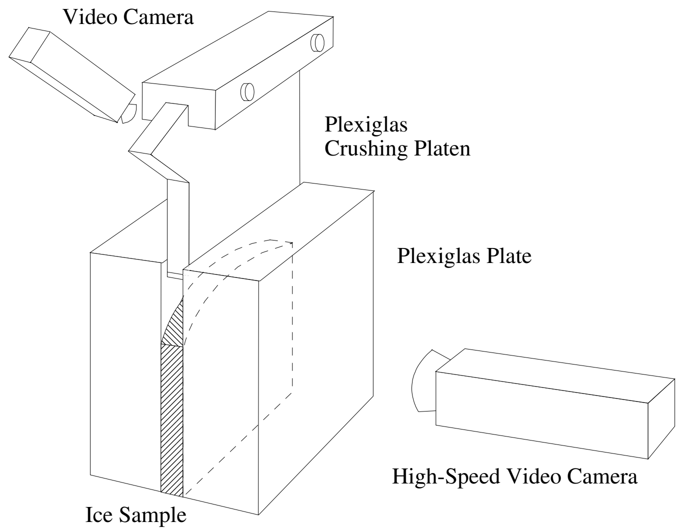

Figure 1a

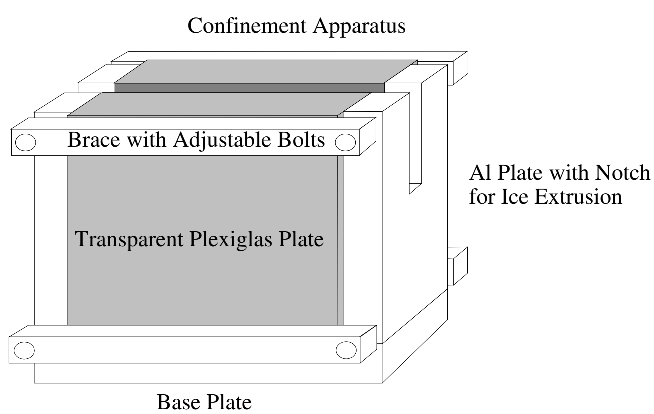

Figure 1b

Figure 1. (a) Conceptual schematic of the ice crushing test method. (b) Details of the ice holder.

provided confinement to the ice sample at the bottom and at the side edges to a height of 6 cm from the bottom. Notches are cut in the upper portion of the side confining plates (above 6 cm) to allow for lateral escape of crushed ice during the tests. Aluminum braces, with adjustment bolts, hold the plates together. The crushing platen was made of Plexiglas and had dimensions 11 cm height x 10 cm width x 1 cm thickness. The platen had a protrusion off to one side that served as a view port through the platen to the ice/platen contact zone for the regular video camera. When the ice holder was mounted and carefully aligned in the MTS test frame, the crushing platen could snuggly slide between the Plexiglas confining plates to make contact with the exposed edge of the ice sample.

A novel pressure sensor was used to measure the pressure at the ice/platen interface (Figure 2). It consisted of a transparent strip of Plexiglas 10 cm long x 1 cm width x 4 mm thickness. The bottom surface of the strip was flat and polished. The top surface was sanded and polished to have a slightly convex shape (approximately 0.45 m radius of curvature) laterally along its whole length (Figure 2b). A load/pressure applied to the bottom of the strip caused it to press against the bottom face of the crushing platen. This leads to some elastic flattening of the curved surface and visible increase in contact width between the strip and the platen at the interface. The view of the ice contact zone was not obstructed by the transparent strip but a small amount of ambient light always reflected off the top surface of the strip. At the places where there was contact between the platen and the strip however, the ambient reflected light would be frustrated and the consequent difference in light contrast would make the contact area between the platen and strip visible. The width of the contact was proportional to the pressure on the bottom face of the strip. The sensor had been calibrated prior to the

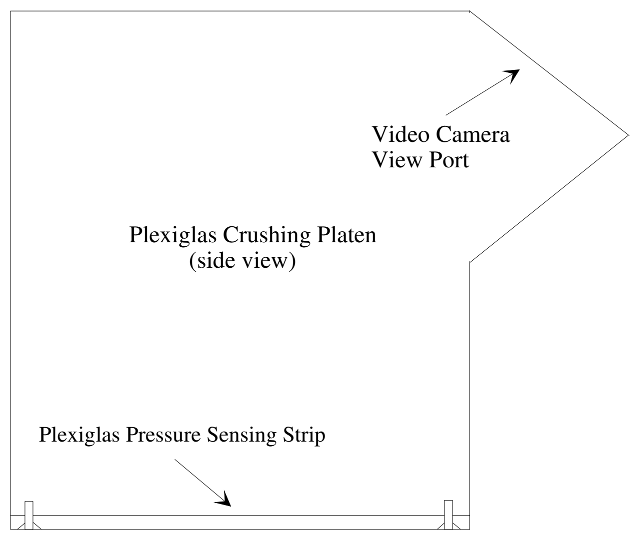

Figure 2a

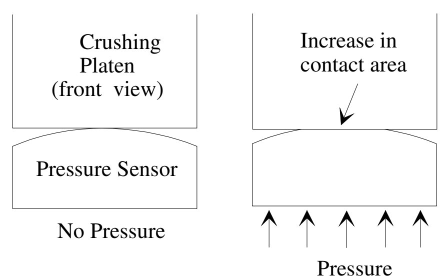

Figure 2b

Figure 2. Schematics of the crushing platen (a) and pressure sensor working principle (b).

tests by pressing it against a stack of 3 plywood pieces that could deform in such a way as to provide uniform pressure over the contacted area. During an ice crushing test the faint image of the platen/sensor contact area would overlie the view of the ice contact zone and would thereby give a map of pressure along the strip for the whole region of platen/ice contact.

For nine of the ten tests conducted the c-axis for the single crystal samples was vertical and in the plane of the ice slab shown in Figure 1. For one experiment the c-axis was oriented at 90 degrees in the plane of the sample from that of the other tests. The crushing platen nominal movement rate was the same for all tests, 10 mm/s. Preparation of the ice samples was critical to insure uniform confinement and has been described in detail by Gagnon (2004). The method of growing the large single crystals has been described by Gagnon (1994a).

A digital high-speed video camera (Lightning RDT™) was used to record the ice behavior during the tests. The image capture rate was 500 frames /s and the resolution of the black and white images was 1280 x 1024 pixels.

ANALYSIS OF A TEST

A series of images, with time stamps, from the video record (Figure 3) show various aspects of Test No.7, a typical well-behaved test. Figure 4 is a reference figure where features of the apparatus and ice behavior discussed below are indicated for the reader's convenience. The image in Figure 4 is the same image in Figure 3 at t = 1.086 s. The load record for the test is shown in Figure 5 with markers (open circles) corresponding to the first 7 video images in Figure 3. Note that we show the record for the time up to just beyond the large shatter event in Figure 3, t = 1.788 s. Beyond this time there is no intact ice contact and the platen begins to penetrate so far into the ice holder as to start restricting the escape of pulverized ice through the egress slots cut in the side plates.

In the following description when a feature of the ice behavior is referred to in an image the feature will have occurred exactly at the time stamp on the image or some time before. This is done for presentation purposes because sometimes the feature in question is more clearly visible in a later image than when it first appears.

When the platen makes contact with the ice, load begins to accumulate (Figure 5). The high-speed video record shows that one of the ice faces usually loses its adherence to the Plexiglas confining plate early in the test. As the loss of adherence progresses a fan-shaped fracture surface appears in the plane of the ice specimen (Figure 3, t = 0.216 s) separating the ice that has adhered to the Plexiglas from the ice that has let go of the Plexiglas. This in-plane fracture continues to extend as the platen moves forward and is tilted about 20-30 degrees from vertical. Linear out-of-plane cracks also begin to appear in a radial pattern centered at the platen/ice contact zone. Eventually the out-of-plane fractures at the sides of the image lead to complete separation of pieces from the ice specimen near the peak in load at around t = 0.266 s in the test (just after the first image in Figure 3).

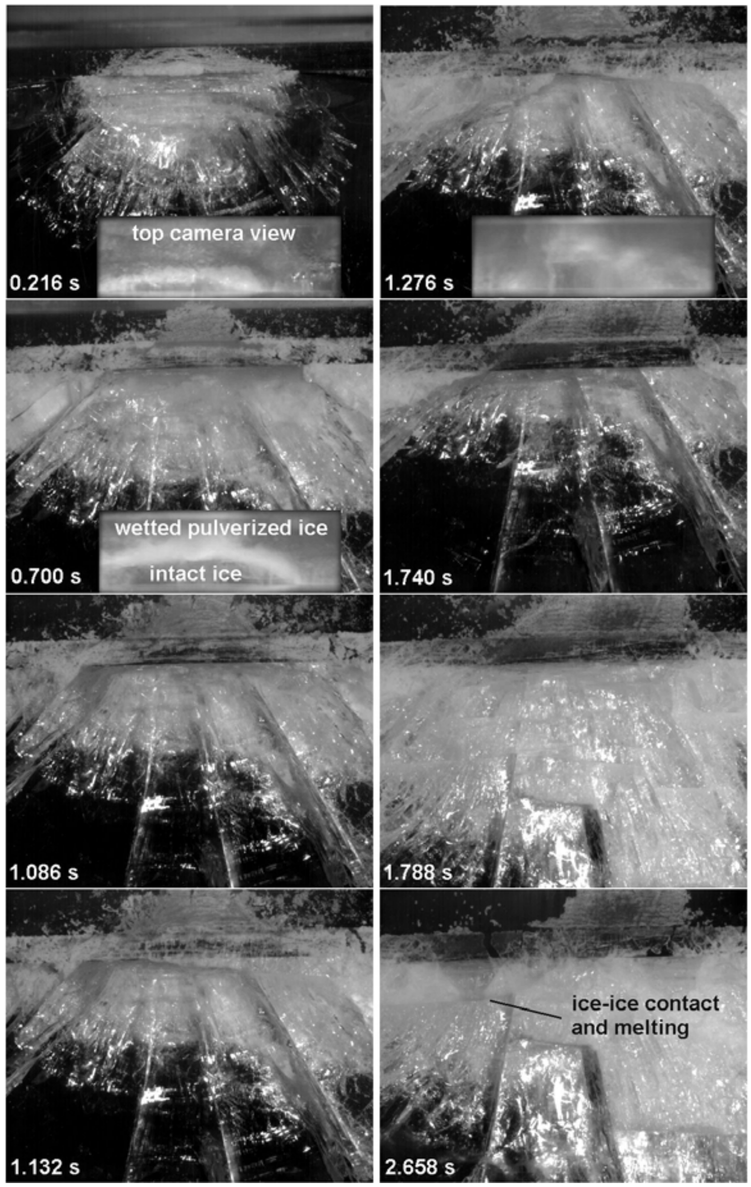

Figure 3. High-speed digital images (with time stamps) from a typical well-behaved test. The ice slab is in the plane of the image and the view is through a Plexiglas plate as shown in Figure 1. Images of the platen/ice contact from the top camera are inset (to scale) on three of the high-speed images. The test was conducted at -10^{o}C.

Apparently the portion of the ice sample on the backside of the large in-plane fracture (relative to the camera), with the face that has lost adherence to the Plexiglas, is more susceptible to fracture-generating stresses. This arises because in-plane lateral confinement is no longer provided by adherence to the Plexiglas or by attachment to the rest of the ice, due to the in-plane fracture. Consequently this ice portion shatters and is pulverized as the platen moves ahead. In the video record the pulverized ice can be seen flowing away to the left and right from the central region of the ice specimen, where the pressure is higher. The remaining ice on the front side of the in-plane fracture stays relatively intact however and as the platen moves further the size of the intact region, visible through the view port on the edge of the crushing platen (Figure 1), increases (Figure 3, insets at t = 0.216 and 0.700 s). The increase in size of the intact contact area with penetration is a reflection of the shape of the intact ice segment created when the in-plane fracture occurred. As discussed below the record from the pressure sensor indicates that the pulverized ice provides a varying degree of confinement that probably helps the intact ice remain in its undamaged state.

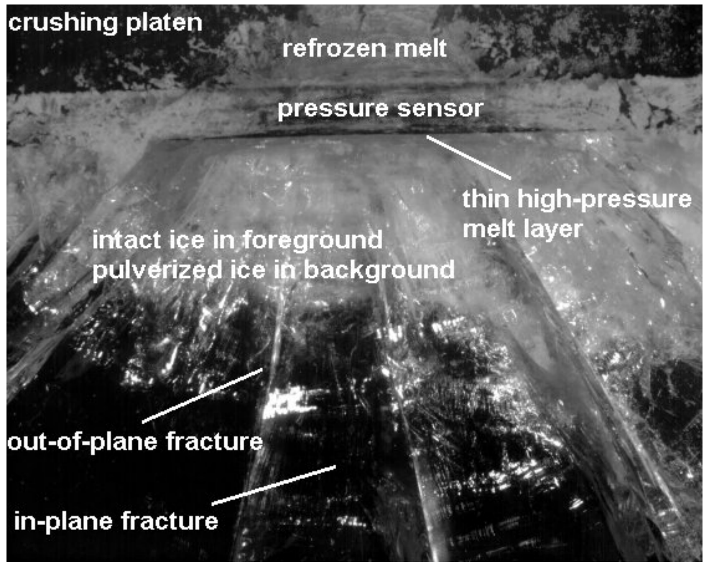

Figure 4. Image from the high-speed video record indicating various aspects of the apparatus and ice behavior. The image is the same as that shown in Figure 3, at t = 1.086 s.

During the time t = 0.25 - 0.48 s in the test spalling from the back and sides of the intact ice contact is visible, each spall corresponding to a drop in load in the sawtooth pattern of load. The test then enters a period of seemingly continuous penetration where spalls, if present at all, are very tiny (both video records) and the load record is relatively smooth. At t = 0.95 s the pronounced spall/load drop activity resumes. The process of spalling, and consequent shaping of the intact ice contact, is illustrated at t = 1.276 s in Figure 3 where the image, and inset image, show spalls at the sides of the

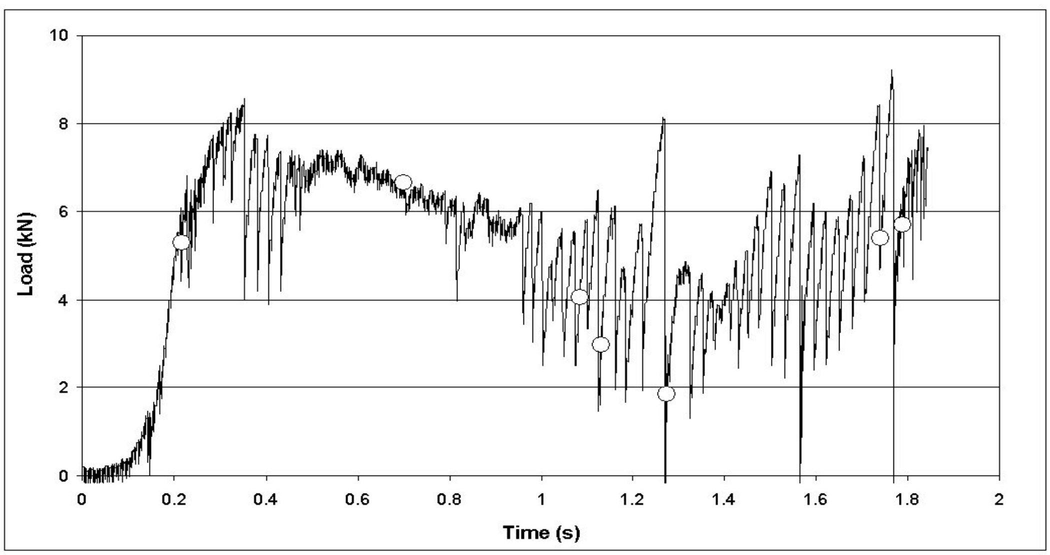

Figure 5. Load record for the test shown in Figures 3 and 4 with markers (open circles) corresponding to the first 7 video images in Figure 3.

central intact ice. Smaller spall events continue and, due to the broadening shape of the impinging intact ice, the area of contact with intact ice increases (Figure 3, t = 1.740 s) until eventually the load, and contact area on intact ice, reach high values and a large portion of the remaining intact ice completely shatters at around t = 1.77 s (Figure 3, t = 1.788 s). Following that, the load record becomes relatively smooth again and steadily increasing because the platen penetration into the ice holder begins to restrict the flow of ice debris out to the side exit notches.

While the shattered and pulverized ice is removed from the contact zone by simply flowing away, a dramatically different mechanism accounts for the removal of intact ice at the ice/platen contact, namely melting. This is evident in the video record that shows a thin layer of liquid extruding from between the platen and ice interface (Figures 3 and 4). The liquid aspect of the layer is evident in that it can be seen wetting the pulverized material adjacent to the sides and behind the intact ice. The liquid can also be seen flowing from between the ice and the platen into the narrow gap between the crushing platen and the Plexiglas plate in the plane of the image (Figures 3 and 4), where it then refreezes. Similar observations were made by Gagnon (2004) during the first series of tests using the same ice holder with a metal crushing platen.

It is interesting that there are occasions in the tests when ice-ice contact occurs and the same process of liquid generation at the contact is evident, along with spalling behavior. This was visible near the end of the test under consideration some time after the shattering of the large portion of intact ice (Figure 3, t = 2.658 s). One of the pieces left over from the shatter event remains in contact with the crushing platen but is sliding to the left as it impinges on some remaining intact ice that contacts it from below. Wetting of surrounding material at the contact region is evident, as are some spalls from the upper ice piece.

The relative movement of the platen against the ice is continuous for a portion of the record shown (t = 0.5 - 0.8 s), that is, at the nominal test rate of 0.010 m/s. In other time segments, where spalls break away from the intact ice/platen contact area that cause abrupt substantial load drops to occur (e.g. t = 0.29 -0.48 s and t = 0.96 -1.75 s), the penetration rate at each load drop is momentarily much higher due to the release of elastic stress in the system. The high-speed video record shows that all abrupt drops in load seen in the load record are caused by spalls either at the sides or at the back of the intact ice contacting the crushing platen. For example a large load drop was caused by the spall at the left shown at time t = 1.276 s (Figure 3).

Due to the high resolution of the digital images, and the close-up view, we can estimate directly from the high-speed video images the compliance of the ice/apparatus system, and the rate of penetration during the load drops induced by the spall events. Using the large load drop at t = 1.25 s the video record indicated that during the ascending portion of the sawtooth approximately 0.16 mm melted off the top of the intact ice as the load increased by 5.566 kN. The corresponding actuator displacement was 0.46 mm. Hence the ice/apparatus system was elastically compressed by 0.46-0.16 mm = 0.30 mm for a change in load of 5.566 kN. This yields a compliance of 5.39×10^{-8} m/N. On the sharp descending side of the sawtooth the load dropped by about 6.88 kN in about 0.3 ms. Hence, using the compliance, we see that the platen moved against the ice 3.71×10^{-4} m in 0.3 ms, that is, at a rate at ~ 1.24 m/s during the load drop, that is, over 100 times the nominal penetration rate! Alternatively the penetration at the load drop can be measured off the images to yield a similar penetration rate.

We attach significance to spalling because it is known to be a major factor in the behavior of ice impact and indentation. The characteristic sawtooth pattern in load records from ice indentation tests (Michel and Blanchet, 1983; Evans et al., 1984; Määttänen, 1983; Timco and Jordaan, 1988; Sohdi and Morris, 1984; Joensuu and Riska, 1988, Frederking et al., 1990), and shape evolution of the ice contact, stems from spalling at the high pressure ice/indentor contact region (Gagnon, 1999). Numerical simulations with just spalling (Daley, 1991) and spalling with granular extrusion (Daley, Tuhkuri and Riska, 1996) support the spalling explanation for the sawtooth pattern.

The novel pressure sensor provided an intriguing record of pressure distribution over the contact area for the duration of tests. Space permits only a cursory discussion. Some general characteristics of the ice behavior can be summarized as follows. Any time that intact ice spanned all or most of the sensor width (Figure 6, center of bottom image), the sensor would contact the full thickness of the platen, i.e. it 'maxed out', indicating an average pressure of at least 30 MPa. On the other hand the pressure could vary considerably when the sensor was over pulverized ice. For example, when pulverized ice lay on top of intact ice the pressure increased as the pulverized ice thickness decreased with the upward movement of the intact ice. Also, pulverized ice pressure was generally less at the sides of the contact zone than in the center (e.g. right side of images in Figure 6). A related observation, was that pulverized ice debris would always flow from regions where the sensor indicated higher pressure to regions of lower pressure.

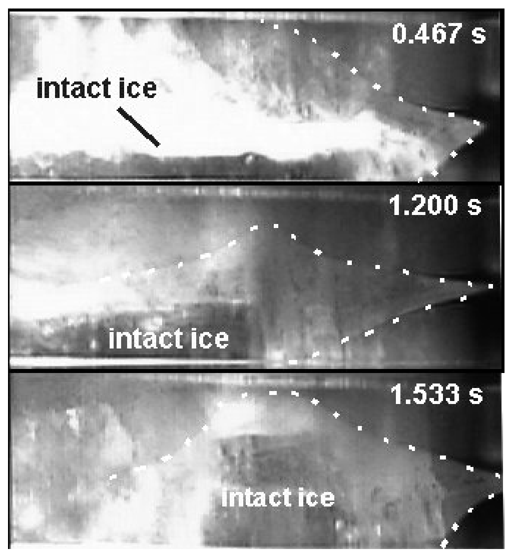

Figure 6. Three images from Test No. 1 showing pressure distribution overlying the ice contact. Sensor contact with the platen is outlined. Intact ice (dark) is labeled while the rest of the view is pulverized ice. The height of each image is the thickness of the platen, 1 cm.

Another factor that seemed to affect the pressure in pulverized ice was its degree of wetness from liquid produced in high-pressure intact ice zones. Images from Test No. 1 (Figure 6) illustrate this phenomenon. It was also observed in two other well-behaved tests that showed intact ice at the beginning and throughout a substantial part of the test. In these tests shortly after contact of the platen with the ice was first made there would be a thin area of intact ice visible against the Plexiglas side plate facing the high speed camera (Figure 6, top image). The rest of the contact was pulverized ice (top image). The average pressure across the mixed material contact was maximum, that is, at least 30 MPa, because the contact between the sensor and the crushing platen spanned the full width of the sensor, implying at least 30 MPa for the pulverized ice and intact ice at that time. With further platen penetration, however, the intact ice thickness (its height in the middle image) increased because it was wedge-shaped, as mentioned above, but the pressure sensor indicated a lower average pressure across the width of the sensor (left of middle image). This implied that the pressure on the pulverized ice had diminished considerably (< 5 MPa) during that time interval since the contact thickness of the intact ice was increasing, and the pressure on intact ice was known to be always at least 30 MPa. We speculate that the marked change in pressure (softening) in the pulverized ice was due to the wetting and saturation that occurred from liquid produced at the high-pressure intact ice / platen contact zone, as seen in the video records.

The melting process has been observed before and explained in detail (Gagnon and Mølgaard, 1991; Gagnon 1994a, 1994b; Gagnon and Sinha, 1991). In the region of high-pressure contact between the platen and the intact ice a pre-existing thin layer of liquid on the ice surface (Faraday, 1859), or one that is produced by pressure melting, starts to flow because of the extreme pressure. The viscous flow of the liquid generates heat and additional melting occurs immediately since the liquid layer is in direct contact with ice. The process can happen at relatively slow rates, such as the continuous crushing rate seen in the present load record and also at much faster rates, such as occurs during load drops in the record where the pressure is momentarily higher.

It is interesting that much more spalling / load drop behavior, typical in ice indentation tests, occurred in this test series in comparison to the first test series Gagnon (2004) where relatively little occurred. This is likely due to the greater compliance of the Plexiglas crushing platen (and pressure sensor) in comparison to the metal platen used before. A mechanism responsible for a portion of the energy dissipation, however, is the same in the present and previous studies, namely melting and viscous flow of melt (Gagnon, 1999).

CONCLUSIONS

A new type of ice crushing experiment has been conducted that enables dual-axis viewing perspectives of the ice behavior. A new pressure sensor, with a promising future, has yielded intriguing information about pressure distribution at the ice contact area.

The important phenomena of melting, due to viscous flow of a thin layer of high-pressure liquid at the ice/structure interface, and spalling at the ice contact zone have been observed in unprecedented detail. As in previous crushing experiments, high-speed video has proven to be a very useful data acquisition system and an invaluable tool for interpretation of the results.

It would be very instructive to conduct similar tests at larger scales and under more uniform confinement scenarios.

ACKNOWLEDGEMENTS

The authors would like to thank the Program of Energy Research and Development (PERD), the Canadian Hydraulics Centre (CHC/NRC) and IOT for their support of this research.

REFERENCES

Daley, C. G., “Ice Edge Contact - A Brittle Failure Process Model” Acta Polytechnica Scandinavica, Mechanical Engineering Series No. 100, Helsinki 1991, 92 pp. Published by the Finnish Academy of Technology

Daley, C.G., Tuhkuri, J., and Riska, K., "Discrete Chaotic Ice Failure Model Incorporating Extrusion Effects", Report submited to the National Energy Board by Daley R&E and the Helsinki University of Technology, Nov., 1996.

Evans, A.G., Palmer, A.C., Goodman, D.J., Ashby, M.F., Hutchison, J.W., Ponter, A.R.S. and Williams, G.J. 1984. Indentation spalling of edge-loaded ice sheets. IAHR Ice Symposium, Hamburg, 113-121.

Faraday, M. 1859. On regelation, and on the conservation of force. Phil. Mag. 17, 162-169.

Fransson, L., Olofsson, T. and Sandkvist, J. 1991. Observations of the Failure Process in Ice Blocks Crushed by a Flat Indentor. Proceedings of the 11th International Conference on Port and Ocean Engineering Under Arctic Conditions, St. John's, Canada, Vol. 1, 501-514.

Frederking, R., Jordaan, I.J. and McCallum, J.S. 1990. Field Tests of Ice Indentation at Medium Scale, Hobson's Choice Ice Island, 1989. Proceedings of the 10th International Symposium on Ice (IAHR 90), Espoo, Finland, Vol. 2, 931-944.

Gagnon, R. 2004. Side-Viewing High-Speed Video Observations of Ice Crushing, Proceedings of IAHR 2004, St. Petersburg, Russia, Vol. 2, 289-298.

Gagnon, R.E. 1994a. Generation of Melt During Crushing Experiments on Freshwater Ice. Cold Regions Science and Technology, Vol. 22, No. 4, 385-398.

Gagnon, R.E. 1994b. Melt Layer Thickness Measurements During Crushing Experiments on Freshwater Ice. Journal of Glaciology, 1994, Vol. 40, No. 134, 119-124.

Gagnon, R.E. 1998. Analysis of Visual Data from Medium Scale Indentation Experiments at Hobson's Choice Ice Island. Cold Regions Science and Technology, Vol. 28, 45-58.

Gagnon, R.E. 1999. Consistent Observations of Ice Crushing in Laboratory Tests and Field Experiments Covering Three Orders of Magnitude in Scale. Proceedings of the 15th International Conference on Port and Ocean Engineering under Arctic Conditions, POAC-99, Helsinki, Finland, Vol. 2, 858-869.

Gagnon, R.E. and Mølgaard, J. 1991. Evidence for pressure melting and heat generation by viscous flow of liquid in indentation and impact experiments on ice. Proceedings of the IGS Symposium on Ice-Ocean Dynamics and Mechanics, 1990, New Hampshire, Ann. of Glaciol., 15: 254-260.

Gagnon, R.E. and Sinha, N.K. 1991. Energy Dissipation Through Melting in Large Scale Indentation Experiments on Multi-Year Sea Ice. Proc. of the 10th International Conference on Offshore Mechanics and Arctic Engineering, Stavanger, Vol. IV, Arctic/Polar Technology, 157-161.

Joensuu, A., Riska, K., "Jään ja Rakenteen Välinen Kosketus"(Contact Between Ice and Structure) Helsinki University of Technology, Laboratory of Naval Architecture and Marine Engineering, Report M-88, Otaniemi, 1988. (in Finnish)

Määttänen, M. 1983. Dynamic ice-structure interaction during continuous crushing. CRREL Rep. 83-85.

Michel, B. and Blanchet, D. 1983. Indentation of an S2 floating ice sheet in the brittle range. Ann. Glaciol., 4: 180-187.

Muhonen, A., "Medium Scale Indentation Tests - PVDF pressure measurements, ice face measurements and Interpretation of crushing video", Client Report by Helsinki University of Technology, Ship Laboratory, Feb.20, 1991.

Riska, K., Rantala, H. and Joensuu, A. 1990. Full scale observations of ship-ice contact. Laboratory of Naval Architecture and Marine Engineering, Helsinki University of Technology, Report M-97.

Sodhi, D.S. and Morris, C.E. 1984. Ice forces on rigid, vertical, cylindrical structures. CRREL Rep. 84-33.

Timco, G.W. and Jordaan, I.J. 1988. Time series variations in ice crushing. Proceedings of the 9th International Conference on Port and Ocean Engineering Under Arctic Conditions, Fairbanks, Alaska, 13-20.

Wilson, C.J. 1999. Downloadable movie from the website of the School of Earth Sciences - The University of Melbourne - Australia. Copyright Notice - The University of Melbourne, 1994 - (2000). http://web.earthsci.unimelb.edu.au/wilson/ice1/index.html